



Understanding the formation of metal-oxide based inorganic solids: Assessing the influence of tetrazole molecule

Bharat Kumar Tripuramallu, Ravada Kishore, Samar K. Das *

School of Chemistry, University of Hyderabad, Hyderabad 500 046, India

ARTICLE INFO

Article history:

Received 8 September 2010
Received in revised form 21 December 2010
Accepted 23 December 2010
Available online 30 December 2010

Keywords:

Molybdenum oxide
Tetrazoles
Self-assembly process
Crystal structures

ABSTRACT

The hydrothermal reaction of Cu(II) salt, ammonium heptamolybdate and 4-ptz (5-(4-pyridyl) tetrazole) at different synthetic conditions yields two compounds $[\text{Cu}(4\text{-Hptz})(\text{Mo}_2\text{O}_7)]$ (**1**) and $[\text{Cu}(4\text{-Hptz})_2(\text{H}_2\text{O})_3]_2[\text{Mo}_8\text{O}_{26}]$ (**2**). Both the compounds **1** and **2** are characterized by routine elemental analyses, IR-, thermogravimetric studies and unambiguously characterized by single crystal X-ray crystallography. Compound **1** exhibits a 3D bimetallic oxide framework, constructed from the tetrazoles and $\{\text{CuMo}_2\text{O}_7\}$ oxide phase. The coordination ability of nitrogen atoms in the tetrazole ring makes the ring acting as a template in the formation of $\{\text{Cu}_4\text{Mo}_6\text{O}_{10}\}$ rings, made up of $[\text{Mo}_2\text{O}_7]^{2-}$ anions and Cu(II) octahedra; the stacking of these $\{\text{Cu}_4\text{Mo}_6\text{O}_{10}\}$ rings along crystallographic *c* axis results in the formation of 3D bimetallic oxide framework. Compound **2** consists of infinite octamolybdate chains and Cu-tetrazolate complex cation. The formation of oxide phase under hydrothermal conditions is discussed, giving importance of the role of geometry of the tetrazole ring.

© 2010 Elsevier B.V. All rights reserved.

1. Introduction

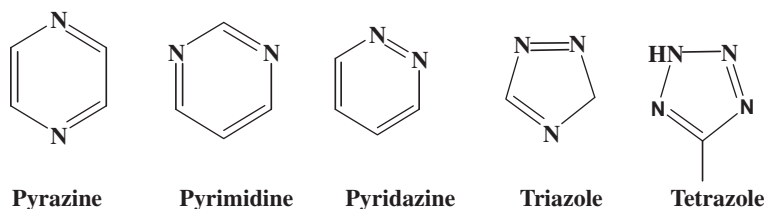
Metal oxide-based solids form an important class of materials because of their promising applications in the contemporary research areas during past several years. A significant research in this area has been directed partly due to interest in their chemistry as well as their applications [1–6]. Molybdenum oxides, that are associated with transition metals, are good candidates for the catalytic applications owing to their structural rigidity. For example, transition metal molybdates of composition MMoO_4 ($\text{M} = \text{Mn}^{2+}$, Co^{2+} , Cu^{2+} and Zn^{2+}) catalyze the oxidative dehydrogenation of propane [7]. Likewise, magnesia supported molybdates are used for anaerobic oxidation of butane to butadiene [8]. MnMoO_4 is used as high capacity anode material for lithium battery [9]. In general, there is a correlation between the complexity of the structure and functionality of the material [10]. The constant evolution of complexity of molybdenum oxides in terms of their functionality requires more knowledge on synthetic strategies to understand the oxide structures [11,12]. One such strategy for the modification of oxide structures involves introduction of organic molecules as structure directors. Zeolites [13,14], biomineralized materials [15], mesoporous oxides [16,17] and transition metal phosphates [18] are the examples in which an organic constituent plays structure-directing role in the constitution of the oxide microstructures. By exploiting

the structure-directing role of polyfunctional organic molecules (for example, organoamine ligands), a wide variety of bimetallic oxides have been isolated and structurally characterized [19–21]. Hydrothermal methods have commonly been used to synthesize the molybdenum oxide-based materials, because this technique offers an excellent route to isolate metastable phases and the reliability of the structure [22,23]. There are two major classes in the M/Mo/O/ligand family of oxides: (i) poloxomolybdate anion clusters, together with secondary metal/ligand components as complexes or cationic networks, constituting metal-oxide-based solids [24,25]; (ii) solids comprising of oxide microstructures rather than anionic clusters to which secondary metal/ligand components are attached to the peripherals of these oxide microstructures. In the later class of inorganic oxides, there are many reports having the general formula $[\text{M}(\text{org})_n\text{Mo}_x\text{O}_y]$ (M = transition metals) in which the bimetallic oxide MMo_xO_y components are 1D chains [26], 2D sheets [27–29] or 3D frameworks [30] to which organoamines are attached *via* coordination through secondary metals as peripheral moieties or bridging subunits. Among these, 3D frameworks, constructed from bimetallic oxides, are quite interesting in terms of both functionality as well as self assembly processes. Zubieta and co-workers have studied structure directing role of the organoamine ligands in the self assembly of bimetallic oxides with the ligands bipyridylamine (bpa), pyrazine (pyz), pyrimidine (pyrd) [30], and 3,4'-bipy, 3,3'-bipy, 4,4'-bipy [31]. Ramanan and his group investigated the influence of 2-aminopyridine on the formation of copper molybdates [32].

As shown in Scheme 1, the pyrazine and pyrimidine have two nitrogen donors, triazole has three nitrogen donors and tetrazole

* Corresponding author. Tel.: +91 40 2301 1007; fax: +91 40 2301 2460.

E-mail addresses: skdsc@uohyd.ernet.in (S.K. Das), skdsc@uohyd.ernet.in (S.K. Das).



Scheme 1. Various polyazaheteroaromatic organic molecules having structure directing roles in the self assembly process of metal-oxide-based solids.

has four nitrogen donors. From the previous reports, it is known that pyrazine and pyrimidine form complex 3D bimetallic oxides CUMO-5 and CUMO-6 with well-defined channels occupied by the pyrazine and pyrimidine units, respectively [30]. These two are rare examples, in which a bimetallic oxide forms a 3D framework and organoamines support the frameworks. As the donor to donor distance is less in both the ligands (pyrazine and pyrimidine), this allows the secondary metal polyhedron of a layer/chain to connect the adjacent layer/chain at shortest distances (through the metal-oxo group) resulting in a 3D bimetallic oxide framework. But in the cases, where the donor to donor distance is more (e.g., 4,4-bipy, dpe, dpa, average N–N distance is 6.52–8.62 Å) [31], these ligands separate the metal polyhedral-layers at largest distances, thereby forming pillared-layered type structures. Interestingly, the ligands pyridazine and triazole (Scheme 1) having adjacent donor sites do not form a 3D bimetallic oxide frameworks, rather, these ligands form a cationic networks in which the oxide clusters are embedded [33,34].

Among these polyazaheteroaromatic compounds (Scheme 1), tetrazoles are of special interest because they consist of all possible bridging fashions for coordinating the adjacent metal centers. The versatility of the tetrazole molecule lies in the availability of more number of donor sites (nitrogen donors). The geometry of these donor sites allows the tetrazole molecule to act as bridging as well as chelating ligands in achieving the desired-networks [35–37]. Due to an availability of four donor sites, it has opportunity to bridge the surrounding secondary metal polyhedra; thus tetrazole molecule with more donor sites can template the formation of oxide network. The only report of tetrazole involving poloxomolybdates, reported by Zubieta and co-workers, has described cationic networks of copper and tetrazoles, in which anionic octamolybdates have been shown to be encapsulated in the channels or voids of the cationic frameworks [38]. In the present study, we have chosen a tetrazole, namely ‘4-ptz’ [5-(4-pyridyl) tetrazole], a tetradentate ligand, to study the influence of the tetrazole molecule on the formation of bimetallic oxide-based new solids, which exploits the geometry of the tetrazole molecule in understanding the self assembly of the bimetallic oxides. We wish to report here the synthesis and structural characterization of two compounds [Cu(4-Hptz)(Mo₂O₇)] (**1**) and [Cu(4-Hptz)₂(H₂O)₃]₂[Mo₈O₂₆] (**2**). In compound **1**, 5-(4-pyridyl) tetrazole (4-ptz) templates the formation of Cu₄Mo₆O₁₀ rings through the all four donor sites, and these rings stack to each other to form a 3D bimetallic oxides, whereas, in compound (**2**) tetrazole forms complex cation [Cu(4-Hptz)₂(H₂O)₃]²⁺ using only one donor N atom, which in turn, is stabilized by the supramolecular interactions with 1D octamolybdate chains [Mo₈O₂₆]_n^{4n−}.

2. Experimental

2.1. Materials and methods

All the chemicals were received as reagent grade and used without any further purification. 5-(4-Pyridyl) tetrazole (4-ptz) was

prepared according to the reported procedure [39]. Elemental analyses were determined by FLASH EA series 1112 CHNS analyzer. Infrared spectra of solid samples were recorded on a JASCO – 5300 FT-IR spectrophotometer as KBr pellets. Thermo gravimetric analyses were carried out on a STA 409 PC analyzer and corresponding masses were analyzed by QMS 403 C mass analyzer, under the flow of N₂ gas with a heating rate of 5 °C min^{−1}, in the temperature range of 30–900 °C.

2.2. Synthesis

2.2.1. Synthesis of the compound [Cu(4-Hptz)(Mo₂O₇)] (**1**)

A mixture of ammonium heptamolybdate tetrahydrate (0.10 mmol, 0.125 g), copper nitrate trihydrate (0.51 mmol, 0.123 g), 4-ptz (0.50 mmol, 0.074 g), and water (555.5 mmol 10.0 g) in the mole ratio 1:5.1:5:5555 was taken; to the resulting reaction mixture, 0.1 mL Et₃N was added and stirred for 30 min. Then the pH of the reaction mixture was adjusted to 1.7 by adding 0.5 M HNO₃. The solution was then transferred to 23 mL teflon-lined autoclave in the stainless steel vessel and heated at 180 °C for 72 h and cooled to room temperature over 2 days to give red block crystals of **1**. Yield: 0.10 g (38%, based on copper) *Anal. Calc.* for C₆H₅N₅CuMo₂O₇ (514.56): C, 14.00; H, 0.97; N, 13.61. Found: C, 14.78; H, 1.01; N, 13.78%. IR (KBr pellet) (ν/cm^{−1}): 3458, 3082, 2920, 2240, 1637, 1516, 1437, 1195, 1022, 850, 760, 634.

2.2.2. Synthesis of the compound [Cu(4-Hptz)(H₂O)₃]₂[Mo₈O₂₆] (**2**)

A mixture of ammonium heptamolybdate tetrahydrate (0.20 mmol, 0.247 g), copper nitrate trihydrate (0.09 mmol, 0.023 g), 4-ptz (0.19 mmol, 0.028 g) and water (555.5 mmol 10.0 g) in the mole ratio 2.22:1:2.11:6172 was taken followed by the addition of Et₃N (0.1 mL) and the resulting reaction mixture were stirred for 30 min. The pH of the reaction mixture was then adjusted to 2.0 by the 0.5 M HNO₃. The solution was then transferred to 23 mL teflon-lined autoclave in the stainless steel vessel and heated at 120 °C for 72 h and cooled to room temperature over 2 days to give blue block crystals of **2**. Yield: 0.04 g (22%, based on copper) *Anal. Calc.* for C₂₄H₃₂Cu₂Mo₈N₂₀O₃₂ (2007.32): C, 14.36; H, 1.61; N, 13.95. Found: C, 13.84; H, 1.42; N, 13.68%. IR (KBr pellet) (ν/cm^{−1}): 3354, 3099, 2096, 1637, 1520, 1385, 1199, 1047, 956, 906, 841, 814, 754, 707, 596, 516, 480.

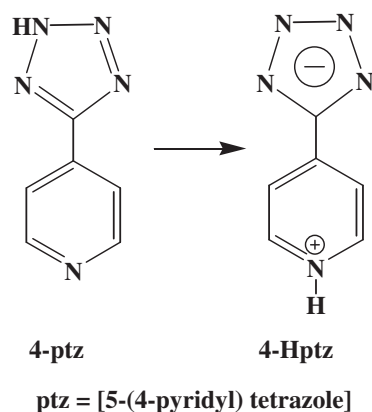
2.3. X-ray crystallography

Data were measured on a Bruker SMART APEX CCD area detector system [λ(Mo Kα) = 0.71073 Å], graphite monochromator, 2400 frames were recorded with an ω scan width of 0.3°, each for 8 s, a crystal detector distance of 60 mm, and a collimator of 0.5 mm. The data were reduced using SAINTPLUS [40], the structures were solved using SHELXS-97 [41] and refined using SHELXL-97 [42]. All non hydrogen atoms were refined anisotropically. We tried to locate the hydrogen atom on the nitrogen atom of the pyridine ring in compound **1** through differential Fourier maps, but did not succeed.

3. Results and discussion

3.1. Syntheses

In the previous report dealing with 5-(4-pyridyl) tetrazole (4-ptz), a cationic network has been shown to be formed by utilizing only two nitrogen's of tetrazole ring and one nitrogen atom of pyridine ring, in which octamolybdates are encapsulated in the voids or channels reminiscent to triazole [38]. In this case, the nitrogen atoms of the pyridine ring of the ligand 4-ptz, can also form coordinate covalent bond with the metal center and alters the formation of oxide structure. The profound influence of the geometry of the 4-ptz ligand can be shown in the oxide structure only by blocking the coordination of the pyridine-nitrogen atom and making availability of the four nitrogens in the tetrazole ring for its coordination (Scheme 2). In the course of our investigation on the synthetic conditions to fulfill these necessities, we have deprotonated the tetrazole ring by adding a base, whereby the negative charge is delocalized in the ring making all the nitrogens available simultaneously for their coordination. To block the coordination of the pyridine nitrogen atom, the concerned reactions were performed at relatively acidic (low) pH, whereby, the pyridine nitrogen gets protonated and blocks its coordination to metal center. This deprotonation–protonation event of the tetrazole ring has profound influence on the formation of oxide structures.



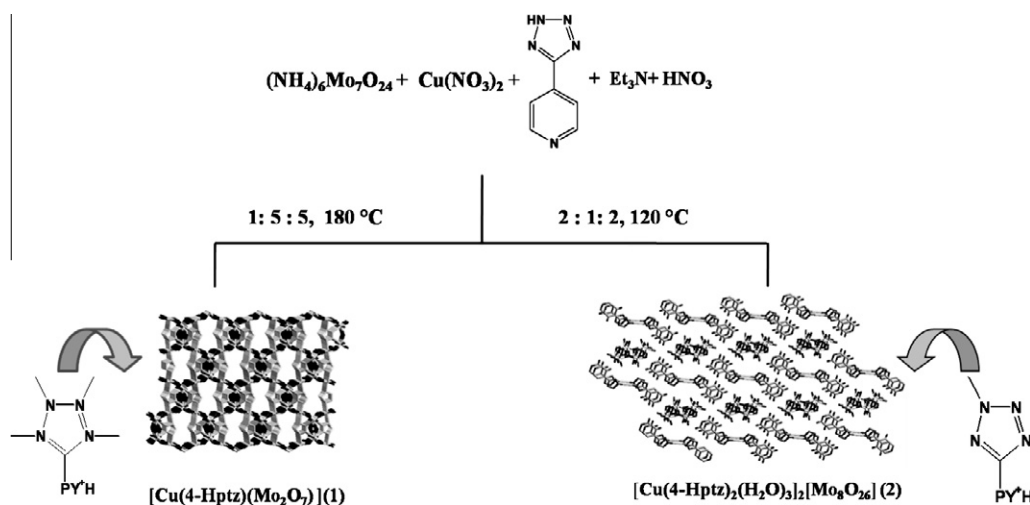
Scheme 2. Schematic representation showing the modification of the ligand to meet the synthetic conditions: formation of zwitter ion.

In a typical synthesis of compound $[\text{Cu}(\text{4-Hptz})\text{Mo}_2\text{O}_7]$ (**1**), a mixture of ammonium heptamolybdate, copper nitrate, 5-(4-pyridyl) tetrazole (4-ptz) and water in the mole ratio 1:5.1:5:5555 was taken and 0.1 mL of Et_3N was added for the deprotonation of tetrazole ring. Subsequently, the pH of the mixture was adjusted to 1.7 by addition of 0.5 M HNO_3 and heated at 180°C for 72 h to give a deep red color block crystals. Compound $[\text{Cu}(\text{4-Hptz})_2(\text{H}_2\text{O})_3]_2[\text{Mo}_8\text{O}_{26}]$ (**2**) was also prepared from the same reactants in the similar synthetic manner, but the mole ratio was changed to 2.22:1:2.11:6172 and temperature to 120°C . Thus, the important variation in the synthesis of compounds **1** and **2** was the variation of mole ratios of the reactants and temperature. In the synthesis of compound **1**, the concentration of ammonium heptamolybdate is less than Cu source and 4-ptz, while in the compound **2**, the molybdate concentration is more. This concentration variation leads to a drastic change in the self assembly process of metal oxides resulting in two completely different structures (namely, compounds **1** and **2**). Finally, the temperature has also remarkable role in stabilizing the structures, for example, compound **1** was prepared at high temperature 180°C , while **2** was prepared at relatively low temperature (120°C). Detailed synthesis and mode of tetrazole binding are shown in Scheme 3. The replacement of base Et_3N with other bases does not give the compounds in the desired yields.

3.2. Description of the crystal structures

3.2.1. $[\text{Cu}(\text{4-Hptz})\text{Mo}_2\text{O}_7]$ (**1**)

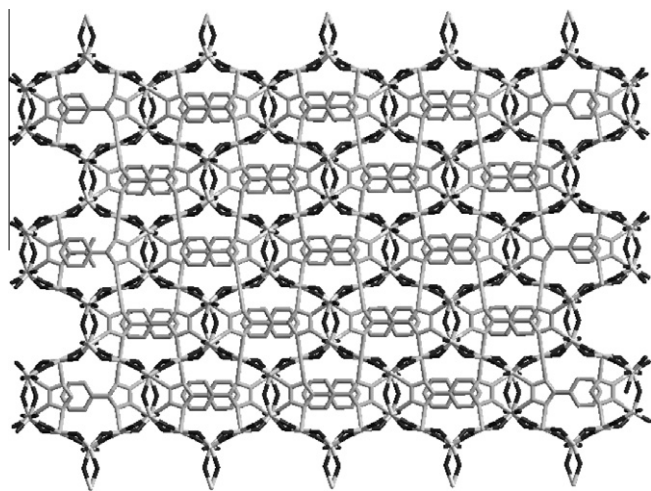
Compound **1** crystallizes in orthorhombic space group $Pnma$; the relevant crystal data and structural refinement for compound **1** are presented in Table 1. As shown in Fig. 1, compound **1** consists of a bimetallic $\{\text{CuMo}_2\text{O}_7\}$ three dimensional network supported by the nitrogen atoms of the tetrazole ring of 4-Hptz. The relevant asymmetric unit consists of one independent Mo atom to which four oxygen atoms are attached (among these, one oxygen is in special position), one Cu atom in special position and half of the 4-Hptz ligand. The molecular formula of the compound from the asymmetric unit is thus described as $[\text{Cu}(\text{4-Hptz})\text{Mo}_2\text{O}_7]$, in which the charge of the dianion $[\text{Mo}_2\text{O}_7]^{2-}$ is compensated by the Cu^{2+} cation. In the ligand 4-ptz, the proton on the nitrogen atom of tetrazole ring is deprotonated, the resulting negative charge is delocalized throughout the ring, while the nitrogen atom of the pyridine ring gets protonated to give a positive charge. Thus, the ligand can be depicted as a neutral ligand,



Scheme 3. Synthesis of compounds $[\text{Cu}(\text{4-Hptz})\text{Mo}_2\text{O}_7]$ (**1**) and $[\text{Cu}(\text{4-Hptz})_2(\text{H}_2\text{O})_3]_2[\text{Mo}_8\text{O}_{26}]$ (**2**).

Table 1Crystal data and structural refinement for compounds **1** and **2**.

	1	2
Formula	C ₆ H ₅ N ₅ CuMo ₂ O ₇	C ₂₄ H ₃₂ Cu ₂ Mo ₈ N ₂₀ O ₃₂
Molecular mass	514.57	2007.32
Crystal system	orthorhombic	triclinic
Space group	Pnma	P1̄
<i>a</i> (Å)	7.466(2)	7.9321(6)
<i>b</i> (Å)	13.030(4)	12.8279(10)
<i>c</i> (Å)	10.910(3)	12.8668(10)
α (°)	90.00	100.11(10)
β (°)	90.00	105.69(10)
γ (°)	90.00	96.69(10)
<i>T</i> (K)	298	100
<i>V</i> (Å ³)	1061.3(5)	1222.11(16)
<i>Z</i>	4	1
<i>D</i> _{calc} (g cm ^{−3})	3.220	2.727
Absorption coefficient	4.363	2.953
<i>F</i> (0 0 0)	980	965
λ (Å)	0.71073	0.71073
Crystal size (mm ³)	0.20 × 0.14 × 0.10	0.34 × 0.16 × 0.08
θ range (°)	2.43–24.97	1.64–25.99
Reflections collected/ unique	8993/969	12556 / 4754
<i>R</i> _{int}	0.1332	0.0216
Refinement method	full-matrix least-squares on <i>F</i> ²	
Goodness-of-fit (GOF) on <i>F</i> ²	1.059	1.187
<i>R</i> ₁ / <i>wR</i> ₂ [<i>I</i> > 2 σ (<i>I</i>)]	0.0426/0.1084	0.0264/0.0729
<i>R</i> ₁ / <i>wR</i> ₂ (all data)	0.0449/0.1122	0.0270/0.0734
Largest difference peak/ hole (e Å ^{−3})	2.067 and −1.296	0.859 and −1.411

**Fig. 1.** 3D packing diagram in the crystal structure of the compound **1** (view along crystallographic *a*-axis).

[5-(4-C₅H₄N⁺H)CN₄[−]](4-Hptz). The dimer [Mo₂O₇]^{2−} consists of two corner sharing {MoO₄} polyhedra with three terminal oxygens of bond lengths 1.763, 1.800 and 1.721 Å, respectively and one bridging μ -oxo with bond length of 1.952 Å. The Mo–O–Mo bridge has a bent configuration with bond angle of 142.0°. The anion [Mo₂O₇]^{2−} extends its dimensionality to 3D by sharing all the three terminal oxygens with another [Mo₂O₇]^{2−} subunit and {CuN₂O₄} octahedron. The two Mo atoms of [Mo₂O₇]^{2−} linked to another unit by the terminal oxygen O1 *via* corner sharing with a distance of 2.202 Å to form a 1D square grid running through crystallographic *a* axis (Fig. 2a). Each molybdenum atom in the dianion [Mo₂O₇]^{2−} is in {MoO₅N} octahedron constructed from the nitrogen atom of the tetrazole ring, three terminal oxygens, one bridging μ -oxo and one

oxygen atom form the other [Mo₂O₇]^{2−} subunit. Each {MoO₅N} octahedron corner-shares with three {MoO₅N} octahedra and two {CuN₂O₄} octahedra. The coordination geometry around Cu(II) atom is defined by the two nitrogen atoms (N2) of two tetrazole rings with bond length of 2.230 Å and four corner sharing oxygen atoms (two O3 and two O4) from two dianions [Mo₂O₇]^{2−} with bond lengths 1.897 and 2.252 Å, respectively. Each {CuN₂O₄} octahedron corner shares with four {MoO₅N} octahedra. The coordination environments of both the metals are shown in Fig. S6 (Supporting Information). From the tetrazole point of view, 4-Hptz is a neutral molecule [5-(4-C₅H₄N⁺H)CN₄[−]](4-Hptz), acting as a tetradentate ligand in which two nitrogen atoms (N1) bind/chelate to one [Mo₂O₇]^{2−} anion and two nitrogen atoms bind/bridge to two copper atoms. The plausible modes of binding with different types of pairs of nitrogen atoms are shown in Table 2. Each tetrazole connects to two Cu octahedra and one [Mo₂O₇]^{2−} anion through four nitrogen donors (Fig. 2b). There are only few instances in which tetrazole exhibits coordination mode of IX [43], in which all the nitrogen atoms of the tetrazole ring are involved in the bonding. In order to meet the available coordination requirements, the ligand 4-Hptz adopts slightly bend conformation from the plane (Fig. S3 in the section of Supporting Information). The covalent connectivity in the {CuMo₂O₇} network brings about a large 20-membered {Cu₄Mo₆O₁₀} ring. Each ring is formed by the two 4-Hptz ligands, whereby the pyridine moiety of each 4-Hptz occupies the cavity of the rings (Fig. 3a). These rings form sheets and these sheets stacked *via* connection through terminal oxygens to form a 3D bimetallic oxide network (Fig. 3b). Two 4-Hptz ligands act as a template in the formation of the {Cu₄Mo₆O₁₀} rings through its coordination *via* nitrogen atom to both Cu and Mo octahedra. It is worth mentioning that the coordination from nitrogen to molybdenum is hardly known in inorganic self-assembled structures. The pattern of chains formed with tetrazole rings and the metal centers are shown in Fig. 4a and the framework of bimetallic oxide {Cu–Mo₂O₇} is shown in Fig. 4b. The arrangement of chains in the framework is shown in Fig. 4c. The selected bond lengths and bond angles of the compound **1** were shown in Table S1 (Supporting Information).

3.2.2. [Cu(4-Hptz)₂(H₂O)₃]₂[Mo₈O₂₆] (**2**)

In our investigation of self assembly process of copper molybdates with tetrazole, we isolated compound **2** at different synthetic conditions, with molecular formula [Cu(4-Hptz)₂(H₂O)₃]₂[Mo₈O₂₆] (**2**). Compound **2** crystallizes in triclinic space group *P*1̄; crystal data and structural refinement for compound **2** are presented in Table 1. The thermal ellipsoid plot for compound **2** is shown in Fig. 5. The relevant asymmetric unit consists of half of the octamolybdate, [Mo₄O₁₃]^{2−} anion and [Cu(4-Hptz)₂(H₂O)₃]²⁺ cation. The crystal structure of **2** consists of infinite molybdenum oxide chains constructed from the corner sharing octamolybdate anions [Mo₈O₂₆]^{4−} and discrete Cu(II) cationic complexes [Cu(4-Hptz)₂(H₂O)₃]. Octamolybdate is well characterized and highly explored POM with α - η isomers [44–50] and has been isolated with different range of organic cations [51], and inorganic metal complexes [52]. In the present study, the octamolybdate chains, formed in the compound **2**, are almost similar with the chains, reported in the compound [(Me–NC₅H₅)₄Mo₈O₂₆] [53]. The monomeric octamolybdate [Mo₈O₂₆]^{4−} unit in the compound **2** comprises of eight edge sharing MoO₆ octahedra. The mode of connectivity of these monomeric octamolybdates gives different types of oxide chains [53]. Each octamolybdate unit in compound **2** consists of four μ^2 -oxo groups, in which each oxo group acts as a linker between two molybdenum atoms from the adjacent subunits to form an infinite oxide chains. The connectivity of a pair of octahedra of one subunit with a pair of octahedra from another subunit through corner sharing (*via* μ^2 -oxo) results in an infinite

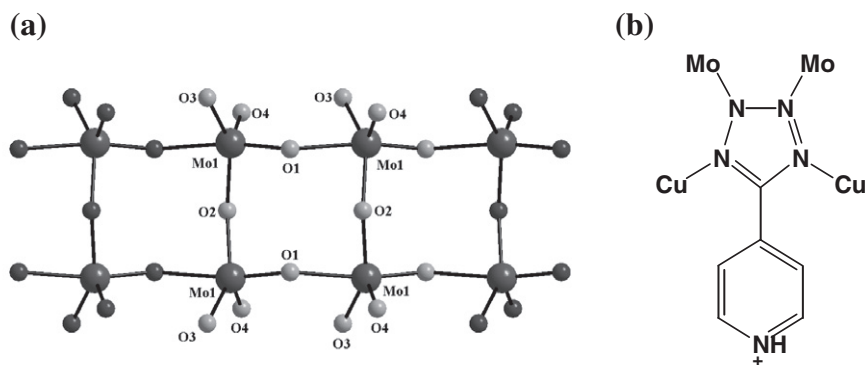


Fig. 2. (a) 1D chain-like arrangement of square grids running through crystallographic *a* axis; (b) coordination of 4-Hptz to the metal centers.

Table 2

Different types of binding modes of nitrogen atom pairs in the [5-(4-pyridyl) tetrazole].

Types of N...N pairs in tetrazole ring	Distance (Å)	Plausible mode of binding	4-ptz
N1–N1*	1.303	Chelating/bridging	
N1–N2	1.329	Chelating/bridging	
N1–N2*	2.151	Bridging	
N1*–N2	2.151	Bridging	
N1*–N2*	1.329	Chelating/bridging	
N2–N2*	2.194	Bridging	
N2,N2*–N3	5.049	Pillaring	
N1,N1*–N3	6.190	Pillaring	

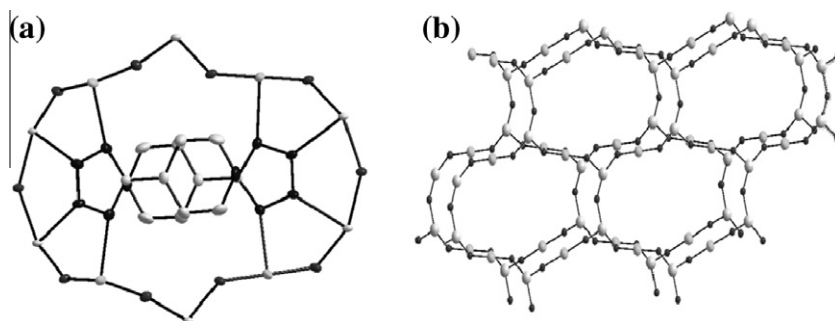


Fig. 3. (a) 20 Membered {Cu₄Mo₆O₁₀} ring, templated by two 4-Hptz ligands; (b) stacking of the bimetallic layers formed from the rings.

1D oxide chains with the formation of rectangular voids of dimension $3.828 \text{ Å} \times 3.862 \text{ Å}$ in the linking region (Fig. 6). The Mo–O–Mo bridges between two subunits are almost linear with an angle of 171.3° , whereas the Mo–O–Mo bridge in the compound **1** is bent with an angle of 142.0° . The cation in the compound **2** consists of Cu(II) centers in {CuO₃N₂} square pyramids. The geometry at each Cu(II) center is defined by one oxygen atom (O16) from one coordinated water molecule in an apical position and two oxygen atoms (O14 and O15) from two more coordinated water molecules and two nitrogen atoms from the two 4-Hptz ligands in the basal plane. In the crystal structure of compound **2**, O14 and O15 atoms suffer from significant disorder problem and they have been split over two positions after fixing their occupancies to 0.5 and 0.5 for O14 and 0.75 and 0.33 for O15. We collected crystal data for compound **2** at liquid nitrogen temperature; however this low

temperature data also did not improve the situation of this disorder problem.

The pyridine nitrogen atom is protonated and does not involve in the bonding as mentioned previously (scheme 2). Only one nitrogen atom of the tetrazole ring coordinates to the Cu atom (Mode-II) [43], whereas in **1** all the four nitrogen atoms are bonded to metal centers. The void space created by the oxide chains are occupied by the Cu(II) cationic complexes (see Fig. S4 in Supporting Information). The selected bond lengths and bond angles of compound **2** are shown in Table S2 (Supporting Information). The oxygen atoms of the octamolybdate chains are involved in hydrogen bonding interactions with hydrogen atoms of the pyridine ring. Each cation [Cu(4-Hptz)₂(H₂O)₃] is connected to three oxide chains via C–H...O weak interactions as shown in Fig. 7a. Also there exists a weak C–H...N supramolecular interactions between two

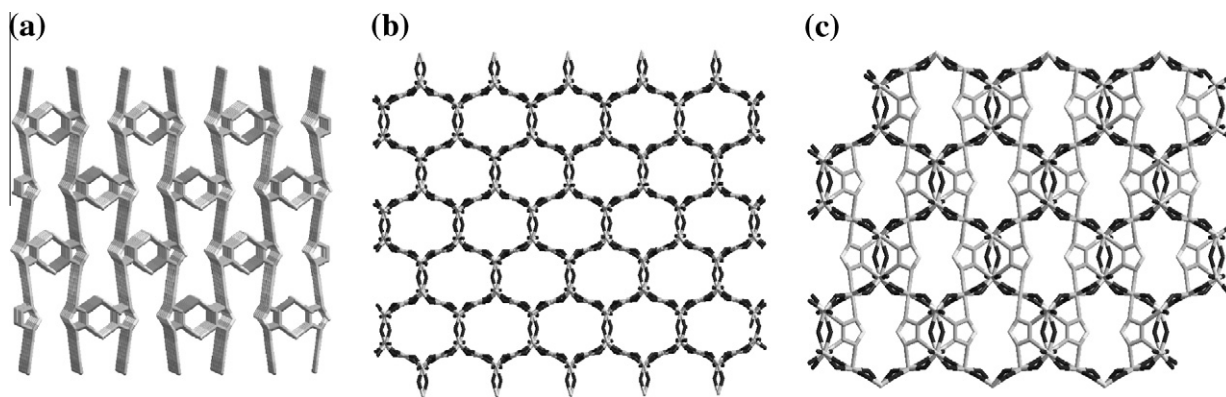


Fig. 4. (a) Cationic chains, formed from 4-Hptz and metal centers; (b) 3D framework of {CuMo₂O₇} bimetallic oxide; (c) fusion of cationic chains in the 3D bimetallic oxide.

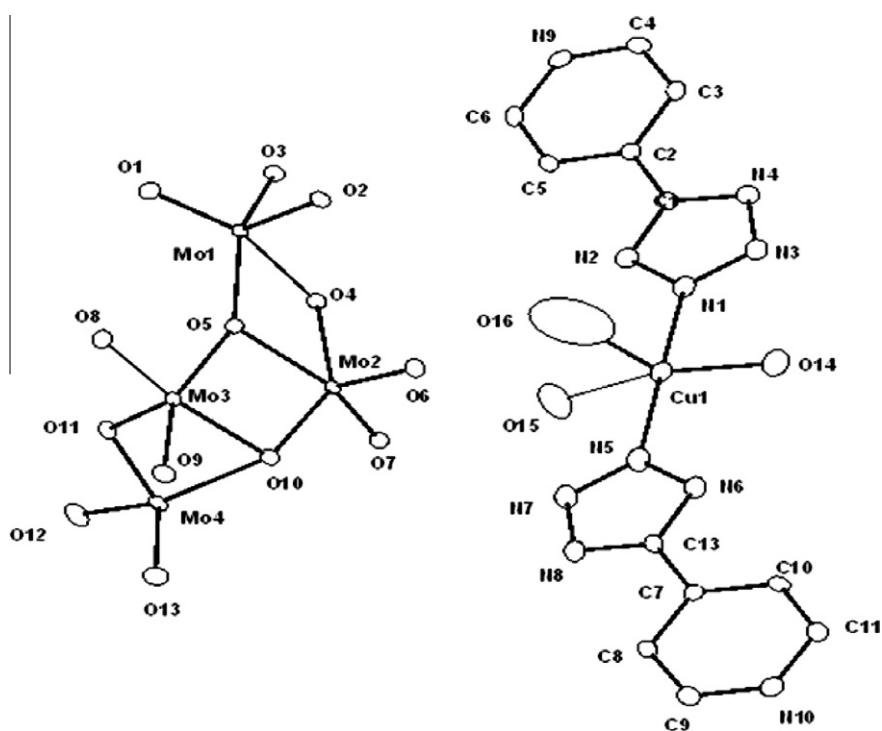


Fig. 5. Thermal ellipsoidal plot of compound 2; hydrogen atoms are not shown for clarity.

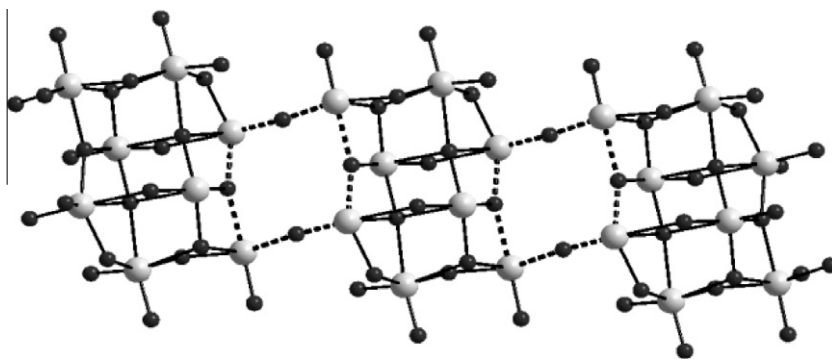


Fig. 6. Infinite octamolybdate chains with rectangular cavities.

[Cu(4-Hptz)₂(H₂O)₃] cations to form a 1D chain as shown in Fig. 7b. Overall the C–H...N interactions form a 1D chain-like structure of [Cu(4-Hptz)₂(H₂O)₃] cations, which in turn, forms 3D framework

with oxide chains through C–H...O interactions (Fig. 7c). The relevant hydrogen bonding distances and angles with symmetry operations are listed in Table 3.

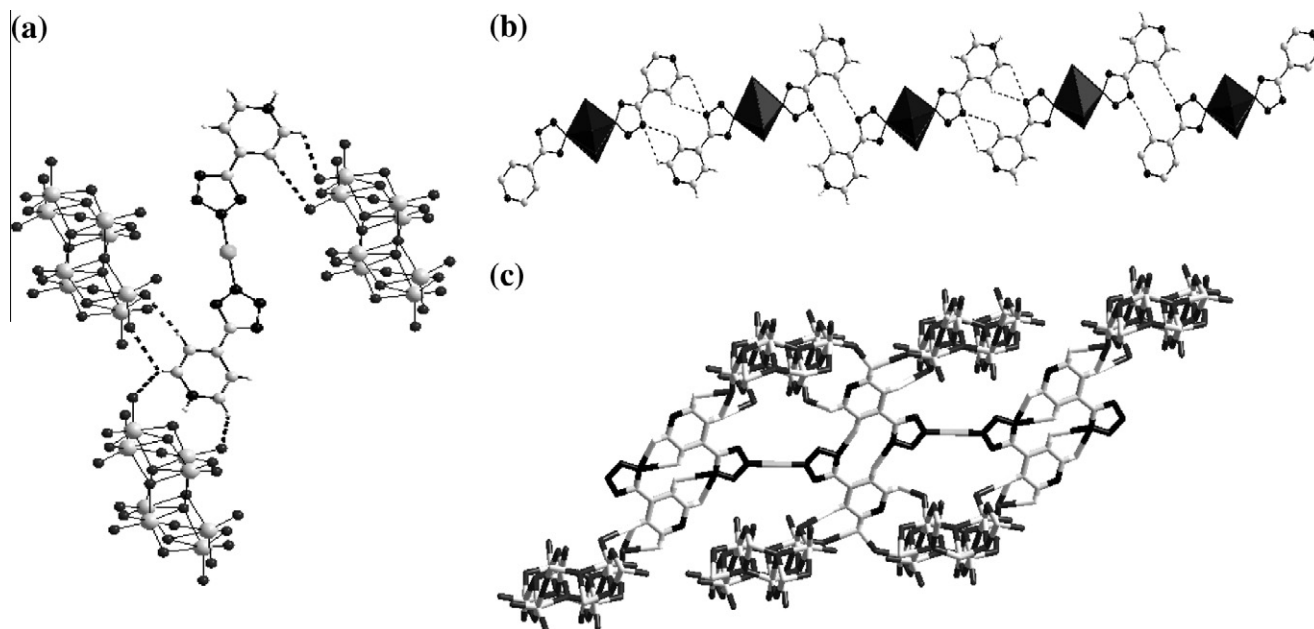


Fig. 7. (a) C–H...O interactions between the 4-Hptz and octamolybdate chains; (b) C–H...N interactions between the two 4-Hptz ligands; (c) overall C–H...O and C–H...N interactions leading to a 3D supramolecular frame work.

Table 3

Geometrical parameters of the C–H...O and C–H...N hydrogen bonds (Å, °) involved in supramolecular network of compound **2**. D = donor; A = acceptor.

D–H...A	d(D–H)	d(H...A)	d(D...A)	∠(DHA)
C(3)–H(3)...O(3)#5	0.93	2.47	3.377(4)	164.0
C(4)–H(4)...O(4)#5	0.93	2.68	3.319(4)	127.0
C(4)–H(4)...O(1)#6	0.93	2.55	3.281(4)	136.1
C(6)–H(6)...O(10)#6	0.93	2.47	3.110(4)	126.3
C(11)–H(11)...O(5)#7	0.93	2.60	3.466(4)	154.6
C(11)–H(11)...O(2)#8	0.93	2.37	2.958(4)	121.0
C(12)–H(12)...O(2)#8	0.93	2.53	3.037(4)	114.3
C(5)–H(5)...N(7)#9	0.93	2.44	3.336(4)	162.5
C(10)–H(10)...N(3)#10	0.93	2.71	3.294(5)	121.5
C(9)–H(9)...N(3)#10	0.93	2.78	3.324(4)	118.3
N(10)–H(10A)...O(12)#11	0.85(5)	1.80(4)	2.634(4)	165(4)
N(9)–H(9A)...O(7)#6	0.86(5)	1.84(5)	2.698(4)	177(4)

Symmetry transformations used to generate equivalent atoms:

#5 $-x+1, -y, -z+1$ #6 $x-1, y, z-1$ #7 $x, y+1, z$ #8 $x+1, y+1, z$ #9 $-x+1, -y+1, -z$
 #10 $-x+2, -y+1, -z+2$ #11 $-x+3, -y+1, -z+2$.

3.3. Thermogravimetric studies

Thermal analyses of both the compounds were performed under nitrogen atmosphere (Fig. 8). Compound **1** shows a thermal stability up to 320 °C and exhibits a weight loss of 28.20% (theoretical: 28.56%) corresponding to the loss of 4-Hptz. A continuous weight loss occurs in the region 352–838 °C to produce an amorphous gray powder. On the other hand, compound **2** shows a thermal stability up to 215 °C and exhibits a weight loss of 35% (theoretical: 34.6%) corresponding to the loss of six water molecules and four 4-Hptz moieties. Compound **1** exhibits more thermal stability than compound **2** due to strong coordination of tetrazole to the inorganic oxide phase leading to a 3D network in compound **1**. The continuous weight losses after the exclusion of 4-Hptz in both the compounds give unknown oxide phases.

3.4. How a tetrazole molecule influences the self assembly process of the inorganic oxides

The availability of more number of donor sites and the geometry of the donor sites in the tetrazole ring allows to show an impor-

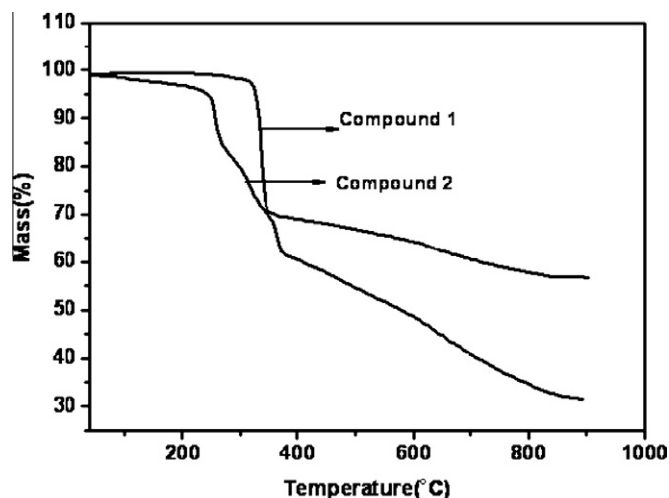
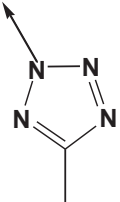
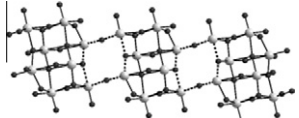
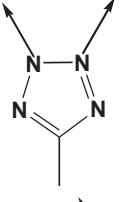

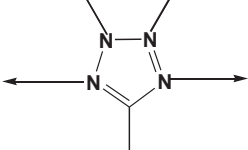
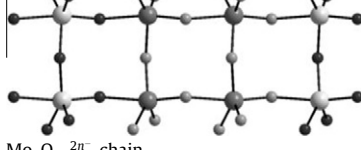


Fig. 8. Thermogravimetric curves for the compounds **1** and **2**.

tant role in the self assembly process of the inorganic oxides. The higher reacting ability and higher oxidation state of molybdenum tend to form the mononuclear, polynuclear or oligomeric anionic cluster anions such as $[\text{MoO}_4]^{2-}$, $[\text{Mo}_2\text{O}_7]^{2-}$ and $[\text{Mo}_8\text{O}_{26}]^{4-}$. The formation of these anionic clusters in the self assembly process of inorganic oxides is mainly dependent on the secondary metal coordination preferences, geometry and availability of the donor sites in the organoamine ligands, and synthetic conditions like pH, temperature and concentration of the reactants. Tetrazoles are known to adopt at least nine distinct types of coordination modes with metal ions in the formation of metal–organic frameworks (see Scheme 1 in the section of Supporting Information) [43]. The geometry of tetrazole ring is unique in the sense that the nitrogen atoms can act as both chelated and bridging components (Table 2). N-containing ligands involve in the self assembly process of inorganic oxides only through the coordination to the secondary metal ions but not to the Mo metal center. The delocalization of negative charge in the ring of tetrazole, gives the ring an aromatic sextet (see Scheme 2 in Supporting Information) [54],

Table 4

Coordination modes of tetrazole and corresponding oxide phases formed in the compounds synthesized/reported.

Coordination mode of tetrazole ^a	Oxide phase	Description of structure
	 Infinite β -octamolybdate chains	Ion pair compound
	 β -Octamolybdate anions	2-D, 3D networks in which octamolybdate anions are encapsulated [38]
	 $\text{Mo}_2\text{O}_{7n-2n-}$ chain	3D bimetallic oxides to which tetrazoles are attached via nitrogen atoms

^a Pyridine moieties are not shown.

thereby enhances the coordination ability of the nitrogen atoms of the tetrazole ring. Due to more coordination ability of the nitrogen atoms in the tetrazole ring allows to coordinate to both secondary metal and molybdenum metal centers. This factor makes a tetrazole molecule different from the other nitrogen containing ligands in the self assembly process. As a result, in the compound **1**, tetrazole ring coordinates to two molybdenum centers and thereby prevents the formation of oligomeric anionic clusters from $[\text{Mo}_2\text{O}_7]^{2-}$ anion. However, in the case of compound **2**, due to more concentration of heptamolybdate (see Section 3.1), tetrazole ring does not prevent the formation of the oligomeric anionic clusters and thereby tetrazole acts as monodentate ligand. The formation of the octamolybdate chains in compound **2** is not purely dependent on the influence of the tetrazole ring; however, the formation of copper complex cation with tetrazole is an important factor, responsible for the formation of the oxide phase. The coordination modes of the tetrazole ring to the metal centers in both the compounds have been shown in Fig. S6 (Supporting information). This profound influence of tetrazole ring in the formation of oxide phases is only possible when the entire donor sites are available for binding. The mode of the tetrazole ring and the corresponding oxide phase in the compounds synthesized/reported are shown in Table 4.

4. Conclusion

Inorganic oxides represent the most important class of materials as far as stability and application aspects are concerned. In order to investigate the self assembly process of bimetallic inorganic oxides involving tetrazole, herein, we have identified 3D covalently linked material $[\text{Cu}(4\text{-Hptz})\text{Mo}_2\text{O}_7]$ (**1**) and 1D compound $[\text{Cu}(4\text{-Hptz})(\text{H}_2\text{O})_3]_2[\text{Mo}_8\text{O}_{26}]$ (**2**). The attractive feature of this article is that in the compound **1**, tetrazole ring, with the aid of four donor sites, templates the formation of the $\{\text{Cu}_4\text{Mo}_6\text{O}_{10}\}$ rings, which stacks further to give a 3D bimetallic oxide framework of $\{\text{CuMo}_2\text{O}_7\}_n$. The coordination ability of the nitrogen atoms in the tetrazole ring to coordinate with both transition metal and

molybdenum metal center in compound **1** favors the formation of the 3D bimetallic oxide. Whereas, in the compound **2** due to more heptamolybdate concentration, tetrazole ring does not play any role to control the oxide phase, and acts as only monodentate ligand. By tuning the synthetic conditions, tetrazole tends to exhibit different coordination modes which can alter the formation of oxide phase. This system not only proves to be a good example to investigate self assembly process and provides more information of the directional syntheses of the inorganic oxide phases, but also offers a fundamental approach of how a nitrogen donor containing organic molecule (tetrazole) influences the self assembly process of the inorganic oxides. Introducing the tetrazole derivatives into the poloxomolybdate (POM) matrix adds a new dimension to the POM based materials in terms of designing solids with specific properties. We are now working on various tetrazole type ligands to understand the self assembly in metal-oxide based solids.

Acknowledgements

We thank Department of Science and Technology, Government of India, for financial support (Project No. SR/SI/IC-23/2007). The National X-ray Diffractometer facility at University of Hyderabad by the Department of Science and Technology, Government of India, is gratefully acknowledged. We are grateful to UGC, New Delhi, for providing infrastructure facility at University of Hyderabad under UPE grant. B.K.T. and R.K. thank UGC, CSIR, New Delhi, for their fellowships. We also thank the Centre for Nanotechnology at University of Hyderabad for financial support.

Appendix A. Supplementary material

CCDC 788800 and 788801 contain the supplementary crystallographic data for **1** and **2**, respectively. These data can be obtained free of charge from The Cambridge Crystallographic Data Centre via www.ccdc.cam.ac.uk/data_request/cif. Supplementary data associated with this article can be found, in the online version, at doi:10.1016/j.ica.2010.12.062.

References

- [1] W. Buchner, R. Schliebs, G. Winter, K.H. Buchel, Industrial Inorganic Chemistry, VCH, New York, 1989.
- [2] R.K. Grasselli, Appl. Catal. 15 (1985) 127.
- [3] D.W. Bruce, D. O'Hare, Inorganic Materials, Wiley, Chichester, 1992.
- [4] P.A. Cox, Transition Metal Oxides, Clarendon Press, Oxford, England, 1995.
- [5] A.J. Cheetham, Science 264 (1996) 794.
- [6] G.B. Gardner, Y.-H. Kiang, S. Lu, A. Asgaonker, D. Venketaraman, J. Am. Chem. Soc. 118 (1996) 6946.
- [7] L.A. Palacio, A. Echavarria, L. Sierra, E.A. Lombardo, Catal. Today (2005) 338.
- [8] G.E. Vrieland, C.B. Murchison, Appl. Catal. A 134 (1996) 101.
- [9] S.-S. Kim, S. Ogura, H. Ikuta, Y. Uchimoto, M. Wakihara, Solid State Ionics 146 (2002) 249.
- [10] S.I. Stupp, P.V. Braun, Science 277 (1997) 1242.
- [11] Y. Zhang, J.R.D. DeBord, C.J. O'Connor, R.C. Haushalter, G. Clearfield, J. Zubieta, Angew. Chem., Int. Ed. 35 (1996) 989.
- [12] M.E. Davis, A. Katz, W.R. Ahamad, Chem. Mater. 8 (1996) 1820.
- [13] J.V. Smith, Chem. Rev. 88 (1988) 149.
- [14] C.S. Cundy, P.A. Cox, Chem. Rev. 103 (2003) 663.
- [15] S. Mann, S.L. Burkett, S.A. Davis, C.E. Fowler, N.H. Mendelson, S.D. Seins, D. Walsh, N.T. Whilton, Chem. Mater. 9 (1997) 2300.
- [16] J. Chen, C. Burger, C.V. Krishnan, B. Chu, J. Am. Chem. Soc. 127 (2005) 14140.
- [17] C.T. Kresge, M.E. Leonowicz, W.J. Roth, J.C. Vartuli, J.S. Beck, Nature 359 (1992) 710.
- [18] R. Murugavel, A. Choudhury, M.G. Walawalkar, R. Pothiraja, C.N.R. Rao, Chem. Rev. 108 (2008) 3549.
- [19] P.J. Hagrman, D. Hagrman, J. Zubieta, Angew. Chem., Int. Ed. 38 (1999) 2638.
- [20] D. Hagrman, P.J. Hagrman, J. Zubieta, Comments Inorg. Chem. 21 (1999) 225.
- [21] M.I. Khan, R.C. Nome, S. Deb, J.H. McNeely, B. Cage, R.J. Doedens, Cryst. Growth Des. 9 (2009) 2848.
- [22] M. Yoshimura, K. Byrappa, J. Mater. Sci. 43 (2008) 2085.
- [23] M.I. Khan, S. Deb, R.J. Doedens, Inorg. Chem. Commun. 12 (2009) 1104.
- [24] R.L. LaDuca Jr., R.S. Rarig Jr., P.J. Zapf, J. Zubieta, Inorg. Chim. Acta 292 (1999) 13.
- [25] D. Hagrman, P. Zapf, J. Zubieta, Chem. Commun. (1998) 1283.
- [26] P.J. Zapf, C.J. Warren, R.C. Haushalter, J. Zubieta, Chem. Commun. (1997) 1543.
- [27] K. Pavani, M. Singh, A. Ramanan, S.E. Lofland, K.V. Ramanujachary, J. Mol. Struct. 933 (2009) 156.
- [28] D. Hagrman, R.C. Haushalter, J. Zubieta, J. Chem. Mater. 10 (1998) 361.
- [29] R.-Q. Fang, Y.-F. Zhao, X.-M. Zhang, Inorg. Chim. Acta 359 (2006) 2023.
- [30] D. Hagrman, C.J. Warren, R.C. Haushalter, C. Seip, C.J. O'Connor, R.S. Rarig, K.M. Johnson, R.L. LaDuca Jr., J. Zubieta, J. Chem. Mater. 10 (1998) 3294.
- [31] R.S. Rarig, R. Lam, P.Y. Zavalij, J.K. Ngala, R.L. LaDuca, J.E. Greedan, J. Zubieta, Inorg. Chem. 41 (2002) 2124.
- [32] K. Pavani, A. Ramanan, Eur. J. Inorg. Chem. (2005) 3080.
- [33] D. Hagrman, J. Zubieta, Chem. Commun. (1998) 2005.
- [34] D. Hagrman, C. Sangregorio, C.J. O'Connor, J. Zubieta, J. Chem. Soc., Dalton Trans. (1998) 3707.
- [35] P. Lin, W. Clegg, R.W. Harrington, R.A. Henderson, Dalton trans. (2005) 2388.
- [36] M. Dinca, J.R. Long, J. Am. Chem. Soc. 129 (2007) 11172.
- [37] P. Pachfule, R. Das, P. Poddar, R. Banerjee, Cryst. Growth Des. 10 (2010) 2475.
- [38] S. Jones, H. Liu, C.C. O'Connor, J. Zubieta, Inorg. Chem. Commun. 13 (2010) 412.
- [39] W. Ouellette, H. Liu, C.J. O'Connor, J. Zubieta, Inorg. Chem. 48 (2009) 4655.
- [40] SAINT: Software for the CCD Detector System, Bruker Analytical X-ray Systems, Inc., Madison, WI, 1998.
- [41] G.M. Sheldrick, SHELXS-97, Program for Structure Solution, University of Gottingen, Gottingen, Germany, 1997.
- [42] G.M. Sheldrick, SHELXL-97, Program for Crystal Structure Analysis, University of Gottingen, Gottingen, Germany, 1997.
- [43] H. Zhao, Z.-R. Qu, H.-Y. Ye, R.-G. Xiong, Chem. Soc. Rev. 37 (2008) 84.
- [44] α -Molybdate: V.W. Day, M.F. Fredrich, W.G. Klemperer, W. Shum, J. Am. Chem. Soc. 99 (1977) 952.
- [45] β -Molybdate: A. Kitamura, T. Ozeki, A. Yagasaki, Inorg. Chem. 36 (1997) 4275.
- [46] γ -Molybdate: M.C. Niven, J.J. Cruywagen, J.B.B. Heyns, J. Chem. Soc., Dalton Trans. (1991) 2007.
- [47] δ -Molybdate: R. Xi, B. Wang, K. Isobe, T. Nishioka, K. Toriumi, Y. Ozawa, Inorg. Chem. 33 (1994) 833.
- [48] ϵ -Molybdate: D. Hagrman, C. Zubieta, D.J. Rose, J. Zubieta, R.C. Haushalter, Angew. Chem., Int. Ed. 36 (1997) 873.
- [49] ζ -molybdate: D.G. Allis, R.S. Rarig, E. Burkholder, J. Zubieta, J. Mol. Struct. 688 (2004) 11.
- [50] η -Molybdate: R.S. Rarig, L. Bewley, E. Burkholder, J. Zubieta, Ind. J. Chem. 42A (2003) 2235.
- [51] W.T.A. Harrison, L.L. Dussack, A.J. Jacobson, Acta Crystallogr., Sect. C 52 (1996) 1075.
- [52] Z. Han, Y. Gao, C. Hu, Cryst. Growth Des. 8 (2008) 1261.
- [53] B. Modec, J.V. Brencic, J. Zubieta, Inorg. Chem. Commun. 6 (2003) 506.
- [54] E.O. John, R.D. Willett, B. Scott, R.L. Kirchmeier, J.M. Shreeve, Inorg. Chem. 28 (1989) 893.